IOP Publishing Measurement Science and Technology
Meas. Sci. Technol. **32** (2021) 015301 (10pp) https://doi.org/10.1088/1361-6501/abac88

Confounding effects of temperature in laser-induced fluorescence concentration measurements with iodine vapor

S K Karthick, B Cukurel and I Jacobi

Faculty of Aerospace Engineering, Technion Israel Institute of Technology, Haifa, 32000, Israel

E-mail: skkarthick@campus.technion.ac.il

Received 24 June 2020
Accepted for publication 5 August 2020
Published 21 October 2020

Abstract

Laser Induced Fluorescence (LIF) provides a non-invasive, quantitative measurement of fluorescent tracers in complex mixing flows. The common availability of broad linewidth lasers and their use with iodine vapor tracers raises a significant concern about confounded tracer concentration measurements, due to the strong dependence of iodine fluorescence on both tracer concentration and flow temperature. We model the sensitivity of iodine fluorescent response to temperature fluctuations, especially for flows with significant temperature contrasts to ambient conditions, and establish a temperature uniformity requirement that bounds the relative error in tracer concentration measurements. We show that in a conventional laboratory setup, in order to bound the measured concentration error to about 5%, the relative temperature fluctuations in iodine LIF must be approximately an order of magnitude smaller than the desired measurement resolution of relative concentration fluctuations. Iodine LIF should thus be employed with great caution.

Keywords: laser-induced fluorescence, iodine tracer, jets and plumes, turbulent concentration measurement

(Some figures may appear in colour only in the online journal)

1. Introduction

Laser Induced Fluorescence (LIF) is a classical spectroscopic method utilized to observe specific species concentration in flow [1–3]. LIF operates by measuring the fluorescence of a passive flow tracer and relating that fluorescent signal to the concentration of the tracer. In general, LIF produces measurable signals that are orders of magnitude larger than those of competing scattering techniques, like the Rayleigh and Raman scattering [4]. And LIF can be used to measure specific combustion products, generated within a reacting flow, by using narrow linewidth tunable-lasers [5] and thus has become a valuable tool in combustion flow research. More generally, LIF is widely used for concentration measurements in non-reacting turbulent jets, plumes, and mixing layers [6–8], and can also be used as a flow visualization tool [9, 10], providing high spatio-temporal resolution, and operability in diverse flow environments [11–14].

Cold flow LIF studies typically seed a gaseous flow field with a low concentration tracer gas with a strong fluorescent response, like carbon dioxide [15], oxygen [16], or vapors of toluene [17], acetone [18], sodium [19], or iodine [20]. Tracer gases from other halide and aromatic groups have also been employed, however they pose challenges in terms of fluorescence efficiency and applicability [21, 22]. Iodine vapor is a particularly popular choice due to its low cost, natural sublimation at room temperature, fluorescent excitation (ex) and emission (em) peaks in the visible spectrum ($\lambda_{ex,max} \approx$ 520–540 nm, $\lambda_{em} \approx$ 540–700 nm), and high fluorescence yield, enabling observation without costly image intensifiers or photon multipliers.

Table 1. Examples of iodine LIF concentration measurements in incompressible, turbulent jets and plumes using broad linewidth ($\Delta\lambda_{in} \sim 0.1$ nm) laser light source.

Study	λ_{in} [nm]	T_t/T_r	U [m s^{-1}]	Carrier	Detector
Kido *et al* [58]	532	1.11	< 30	N_2	^iC_S
Kido *et al* [59]	532	1.11	< 13	Ar	^iC_S
Iida & Ando [45]	532	1.11	0.3	He,N_2,CO_2	^iC_S
Kido *et al* [60]	532	0.71	< 30	Ar	^iC_S
Muruganandam *et al* [24]	532	1.03	< 6	air	C_S
Wu *et al* [25]	532	1.22	< 2.5	N_2	C_S
Wu *et al* [26]	527	1.22	< 2.5	N_2	C_S
Xu *et al* [27]	527	1.22	< 2.5	N_2	C_S

C_S—CMOS/CCD camera sensor, ^iC_S—intensified CCD camera sensor

Iodine vapor was first used as a LIF tracer by Hiller & Schmidt-Ott (1977) [9] for flow visualization of low density gas-jets. Since then, iodine vapor has been employed for flow visualization over a wide range of flow regimes: subsonic [23–27], transonic [4, 28], supersonic [10, 29, 30], hypersonic [31, 32], and rarified flows [33, 34]. Iodine vapor was also used to make quantitative measurements of flows, including pressure [35–38], velocity [10, 14, 39], temperature [37, 40–42], and scalar concentration fields [23, 37, 43–47].

The primary challenge with iodine LIF is the temperature sensitivity of both its vapor saturation behavior and its fluorescence response. The saturation concentration of iodine vapor in air (calculated via Antoine's equation [48, 49]) is far more sensitive to changes in temperature than other fluorescent tracers (like UV responsive acetone and toluene [50, 51]), raising the possibility of local sublimation or condensation of the tracer and thus corruption of any concentration measurements. Independent of the saturation behavior, the fluorescence response of iodine vapor is also highly sensitive to small changes in temperature, T, and pressure, p. Because the scalar concentration is inferred from the fluorescence response, this temperature dependence can significantly confound LIF concentration measurements: variations in temperature will manifest themselves in the fluorescence response indistinguishably from variations in actual concentration, especially when broad linewidth laser light source is used for excitation.

The standard approach to ameliorating this temperature dependence in the fluorescent response has been the use of narrow linewidth (incident $\Delta\lambda_{in} \sim 0.001$ nm), tunable-dye lasers. For compressible flows or flows with non-uniform temperature, i.e. where the total temperature of the flow, T_t, is different from the ambient reference temperature, T_r, narrow linewidth lasers can be tuned to select a temperature- or pressure-independent absorption linewidth of iodine [22, 38]. The selected absorption line determines the temperature dependency of the Boltzmann population fraction responsible for the fluorescence signal [52], thereby eliminating the confounding thermodynamic influence on the concentration measurements [38, 44, 53–55]. However, despite this solution, iodine LIF measurements of concentration are still commonly performed using narrow linewidth laser at excitation wavelengths with known temperature sensitivity, in which temperature variations were simply assumed to be negligible, without reporting a detailed sensitivity analysis [23, 46, 56, 57].

The lack of reported temperature sensitivity analyses in narrow linewidth lasers has likely led to the increased use of even broad linewidth lasers for iodine LIF. Broad linewidth lasers are now a commonplace in many engineering laboratories, for use in particle-image velocimetry and general flow visualization, and these have been widely reported as an excitation source for iodine LIF, as cataloged in table 1, for a variety of flow velocities U, even in non-isothermal systems. These studies highlight a known but often unaddressed question: how much temperature uniformity is actually necessary in an incompressible flow to ensure that temperature variations do not confound concentration measurements? This question has particular urgency with regard to these common, broad linewidth laser light sources used for visible excitation.

In the present study, we examine the coupling between temperature, tracer concentration, and fluorescent response in an idealized, iodine LIF system for incompressible flows using a representative, broad linewidth laser ($\Delta\lambda_{in} \sim 0.1$ nm) with incident wavelength, $\lambda_{in} = 532$ nm, in order to obtain operating guidelines on temperature control for reliable concentration measurements. In section 2, we describe the basic mechanism of LIF concentration measurements with iodine vapor and its temperature dependence; in section 3, we show how tracer concentration measurements can be biased by temperature variations; in section 4 we examine the sensitivity of the fluorescent response to small changes in tracer concentration and temperature, after which, in section 5, we develop a constraint on experimental temperature uniformity to ensure reliable, un-confounded concentration measurements using iodine LIF.

2. LIF concentration measurement with iodine vapor

The basic LIF technique involves exciting the fluorescent tracer with a monochromatic light source near the tracer's specific excitation wavelength, λ_{ex}, measuring the power of the fluorescent response, and associating that response with the

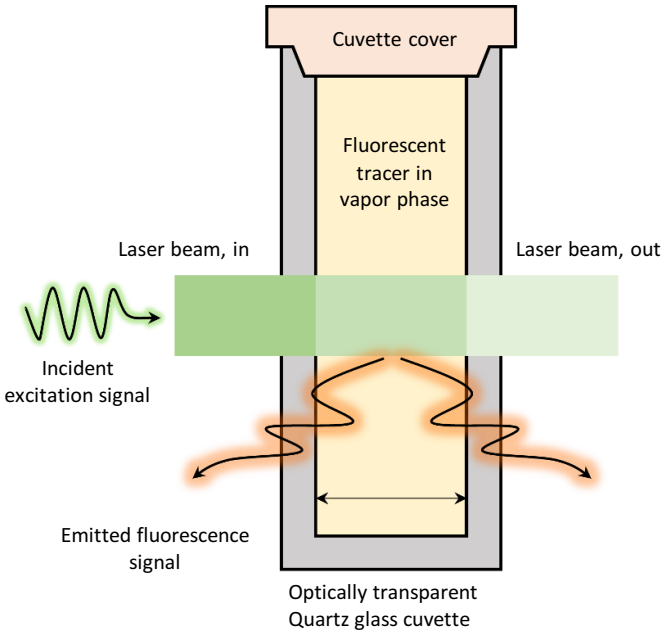

Figure 1. Schematic showing the excitation of fluorescent tracer (in vapor phase) contained in a cuvette with optical path length (l) using an incident laser light source (λ_{in}, P_0), and emission of fluorescence signal (λ_{em}, $P_{f,\text{ideal}}$) from the tracer.

concentration of the tracer itself. A simplified LIF configuration is illustrated in figure 1, where a cuvette of air containing iodine vapor is placed in the path of a laser source emitting at incident power, P_0. That incident power will be absorbed by the iodine, exciting the tracer molecules from the ground state to a higher energy state, and emitting fluorescent light with ideal power $P_{f,\text{ideal}}$ assuming no losses at λ_{em} as the molecules return to their ground state. The remaining power, P, not converted to a fluorescent emission, will pass through the cuvette. The fluorescence power, $P_{f,\text{ideal}}$, serves as a direct measure of local tracer concentration, $C(\vec{x},t)$, where $\vec{x}$ is the local spatial coordinate and t is time, and can be calculated from the difference between incident and transmitted powers:

$$P_{f,\text{ideal}} = P_0 - P \tag{1}$$

The fluorescence power, $P_{f,\text{ideal}}$, can be represented by the light absorbance, A, which is just the logarithmic difference of the incident to transmitted powers

$$A = \log_{10} P_0 - \log_{10} P \tag{2}$$

Applying the Lambert-Beer law then allows us to relate the absorbance to the local tracer concentration, C, the optical light path, l, and an absorptivity factor, $\varepsilon(p,T)$, as:

$$A = -\log_{10}\left(\frac{P}{P_0}\right) = -\log_{10}\left(1 - \frac{P_{f,\text{ideal}}}{P_0}\right) = \epsilon(p,T)Cl \tag{3}$$

Thus we can measure the local tracer concentration by measuring the fluorescent and incident powers,

$$P_{f,\text{ideal}}(p,T,C) = P_0\left(1 - 10^{-\epsilon(p,T)\,Cl}\right). \tag{4}$$

However, the actual fluorescent power, P_f, will differ from the idealized power, $P_{f,\text{ideal}}$, due to energetic losses in the fluorescence system. The nature of these losses is specific to the details of the incident light and the tracer molecule, as explained below.

The incident light source in LIF can have a significant impact on the temperature sensitivity of the resulting fluorescent power. Incident light is never purely monochromatic, and thus is described with a linewidth, $\Delta\lambda_{\text{in}}$ defined by the full-width at half-maximum output intensity of the light source. Similarly, the tracer molecules themselves absorb incident light over a range of wavelengths. Because iodine is a heavy, diatomic species, it contains numerous absorption lines in the visible spectrum [22]. Because the dependence of fluorescence power on pressure (p) and temperature (T) varies by absorption line, specific isolated wavelengths with very small temperature or pressure variation can be targeted with narrow linewidth lasers to excite isolated absorption lines of iodine vapor, as noted above, to ensure that measurements are not significantly biased by changing thermodynamic conditions. However, most lasers commonly available in flow research (e.g. pulsed lasers like Nd:YAG 532 nm, Nd:YLF 527 nm, or continuous lasers like Ar-Ion 514.5 nm, without intracavity etalon, and diode pumped solid-state lasers like DPSS 532 nm) have a broad linewidth ($\Delta\lambda_{\text{in}} \sim 0.1$ nm), making this type of absorption line targeting impossible. Broad linewidth lasers produce fluorescence over multiple wavelengths, including wavelengths that may be highly sensitive to changes in temperature or pressure [58]. But, despite this potential for thermodynamic bias of fluorescence measurements, broad linewidth lasers have still been widely used for measuring iodine concentration (noted above and in table 1).

In addition to the temperature dependence of fluorescent power due to the broad linewidth lasers, there are also natural energetic losses in the fluorescence emission that result in a reduction of the power output (internal conversion, inter-system crossing, vibrational relaxation, phosphorescence, collisional quenching with carrier gas, and self-collisional quenching) [12, 13, 52, 61]. Hence, the actual P_f can be represented in terms of a fluorescence efficiency (or fluorescence yield), $\Phi(p,T)$, that depends on pressure and temperature, such that

$$P_f = \Phi(p,T)P_{f,\text{ideal}} = \Phi(p,T)\,(P_0 - P)\,. \tag{5}$$

The fluorescence efficiency, $\Phi(p,T)$, can be represented in terms of the ratio of the actual emission lifetime of the fluorescence, τ, to its idealized emission lifetime, τ_0, as $\Phi = \tau/\tau_0$ [61]. Quenching (Q) of the florescence (by collision of tracer molecules with themselves or with the carrier gas molecules) reduces the idealized emission lifetime and thus reduces the actual fluorescent power output, P_f. The idealized emission lifetime, τ_0, automatically takes into account non-quenching losses, and can be described in terms of radiative (k_r) and non-radiative (k_{nr}) loss rates, which together sum to Einstein's coefficient for spontaneous emission, A_{21}. Expanding

the fluorescence efficiency in terms of the quenching and non-quenching loss rates yields:

$$\Phi(p,T) = \frac{1/\tau_0}{1/\tau} = \frac{k_r+k_{nr}}{k_r+k_{nr}+Q(p,T)} = \frac{A_{21}}{A_{21}+Q(p,T)} \tag{6}$$

Therefore, taking quenching losses into account, we rewrite the fluorescent power relation, equation (4), in terms of the actual fluorescent power, as:

$$P_f(p,T,C) = \Phi(p,T)P_0\left(1-10^{-\epsilon(p,T)\,C\,l}\right) \tag{7}$$

As before, the fluorescent power is a direct function of concentration, C, but also depends directly on temperature and pressure. In the case of incompressible flow, the static pressure change is typically negligible and hence, the absorptivity and the quenching rate dependence on p can be neglected [37, 38, 41, 49], leaving:

$$P_f(T,C) = \Phi(T)P_0\left(1-10^{-\epsilon(T)\,C\,l}\right) \tag{8}$$

Still, the fluorescent power, temperature, and concentration are coupled, and thus to measure concentration variations alone requires precise knowledge of the extent of this coupling.

3. Concentration and temperature effects on fluorescent power

Measuring concentration as a passive scalar assumes that the concentration varies only in space and time, $C(\vec{x},t)$. However, at saturation conditions, the equilibrium concentration of tracer in vapor form will, in principle, be entirely determined by the local temperature. As the local temperature changes, the saturation concentration of iodine vapor, C_s, will also change (as described by Antoine's equation), causing excess vapor to condense or condensed iodine to sublime, until the new saturation fraction is achieved. In this case, the concentration is just a direct proxy for temperature measurements, with $C(\vec{x},t) = C_s(T(\vec{x},t))$, and for non-isothermal flows, with different Schmidt and Prandtl numbers, the concentration will then reflect some unknown blend of heat and scalar transport effects.

In order for the iodine vapor to behave as a passive scalar, the vapor system must operate below the saturation concentration (to avoid condensation), and in the absence of any additional reservoir of solid iodine (to avoid sublimation). The latter condition can be met in most experiments by regularly cleaning deposited or condensed iodine crystals from the experimental apparatus. Thus, for the remaining analysis we assume that the local concentration varies as a result of mixing, independent of temperature, and therefore focus entirely on the temperature effect with respect to the fluorescence measurement.

In order to model the fluorescent power, P_f, produced in a typical flow system, we need to define a) the range of temperatures, T, and concentrations, C, expected, as well as b) the behavior of the fluorescence efficiency, Φ, and absorptivity, ε.

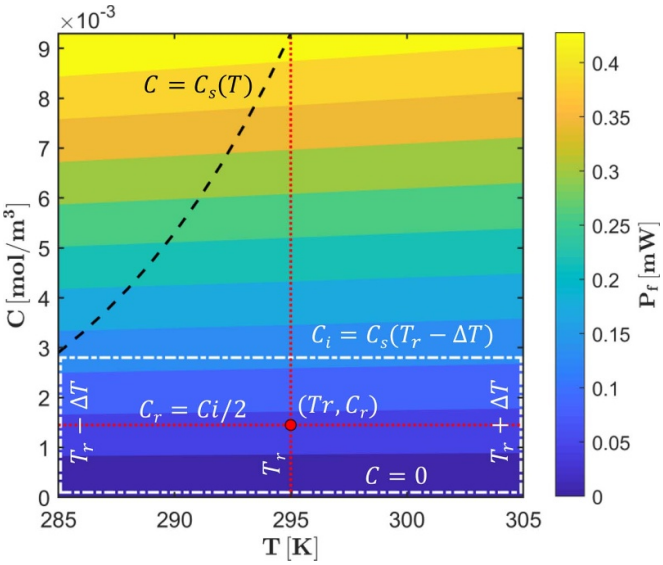

Figure 2. The variation of fluorescence power (P_f) for different values of iodine concentration ($C = [0, C_i]$) and temperature ($T = T_r \pm \Delta T$) encountered in the hypothetical turbulent mixing system. The maximum seeding concentration is at $C_i = C_s(T_r - \Delta T)$, $C_r = C_i/2$ and $\Delta T = 10$ K. The dash-dotted white box represents the feasible operating region expected in typical room-temperature experiments. The dashed black line represents the saturation curve ($C_s(T)$) of iodine vapor. The red, dotted lines mark the reference temperature (T_r) and concentration (C_r).

We consider a hypothetical turbulent mixing system, typical of many systems for which broad linewidth iodine LIF has been used: a turbulent jet seeded with iodine vapor released to a quiescent atmosphere, operating at room temperature (reference temperature $T_r = 295$ K). The temperature expected in this flow, T, varies about the reference temperature by ΔT, such that $T = T_r \pm \Delta T$. The minimum temperature achieved in the system limits the maximum vapor concentration, so we set the inlet vapor concentration, $C_i \leq C_s(T_r - \Delta T)$, such that the system is always below saturation for all possible temperatures, T. The reference concentration, C_r, is then selected as $C_r = C_i/2$, such that the concentration C can range from 0 to C_i.

The fluorescence efficiency and absorptivity functions for the model assume a typical, broad linewidth laser source ($\Delta\lambda_{in} \sim 0.1$ nm, $\lambda_{in} = 532$ nm), like the Nd:YAG laser. The fluorescent yield, Φ, depends on A_{21} and the quenching rate, Q, (in equation (6)) which in turn depends on the molecular properties of the carrier gas and fluorescent vapor, as listed in table 2. The absorptivity, $\varepsilon(T)$, was measured empirically for a carrier-gas-independent iodine system at 532 nm for a broad linewidth laser by Kido *et al* [60]; their data was extracted (from their figure 7) and fit to a linear curve with residues of less than $\pm$ 0.1%, given by:

$$\epsilon(\pm 0.1\%) = -0.348 \cdot (T - 273) + 210 \tag{9}$$

Values of the selected broad linewidth for the visible wavelength lasers in the market are in the range of $\Delta\lambda_{in} \sim 0.05 - 0.1$ nm. Typical values of ε fall within the

Table 2. Representative parameters for modeling fluorescent response.

Symbol	Value	Units	Description
ΔT	10	K	Change in temperature
T_r	295	K	Reference temperature
P_r	101 325	Pa	Reference pressure
C_i	0.002 9	$\text{mol}\cdot\text{m}^{-3}$	Initial concentration ($C_s(T_r-\Delta T)$)
C_r	0.001 5	$\text{mol}\cdot\text{m}^{-3}$	Reference concentration ($C_i/2$)
N_A	6.022×10^{23}	mol^{-1}	Avogadro Constant
k_B	1.381×10^{-23}	$m^2\cdot kg\cdot s^{-2}\cdot K^{-1}$	Boltzmann Constant
P_0	25	W	Average laser power
λ_{in}	532×10^{-9}	m	Wavelength of the incident laser light
τ_0	2×10^{-6}	s	Spontaneous natural life time of I_2 vapors in $\mathbf{X}-\mathbf{B}$ electronic system [22, 61]
$r_{m,c}$	3.94, 25.23	$\times10^{-3}\cdot\text{kg}\cdot\text{mol}^{-1}$	Reduced Atomic mass of the carrier gas: He, N_2 [22, 49]
$r_{m,t}$	126.9	$\times10^{-3}\cdot\text{kg}\cdot\text{mol}^{-1}$	Reduced Atomic mass of the fluorescent tracer gas: I_2 [22, 49]
σ_c	0.15, 3	$\times10^{-20}\cdot\text{m}^2$	Quenching cross section of the carrier gas: He, N_2 [22, 49]
σ_t	65	$\times10^{-20}\cdot\text{m}^2$	Quenching cross section of the fluorescent tracer gas: I_2 [22, 49]
A_{21}	$1/\tau_0$	s^{-1}	Einstein's coefficient for spontaneous emission [22, 61]
n	$p_r/k_\text{B}T_r$	m^{-3}	Total number density per unit volume
Q_c	$n\sqrt{8\pi k_\text{B}T}\left(\frac{\sigma_c}{\sqrt{r_{m,c}/N_A}}\right)$	s^{-1}	Quenching rate due to the presence of carrier gas [22, 49]
Q_t	$n\sqrt{8\pi k_\text{B}T}\left(\frac{0.025\sigma_t C_r}{\sqrt{r_{m,t}/N_A}}\right)$	s^{-1}	Quenching rate due to the fluorescent tracer gas in the mixture [22, 49]
Q	Q_c+Q_t	s^{-1}	Total quenching rate [22, 49]

bounded range for the aforementioned variations in $\Delta\lambda_\text{in}$. Hence, the analysis is expected to be widely applicably for broadband lasers in the visible spectra, although the general method can be easily applied to exceptional laser systems.

Combining the fluorescence efficiency and absorptivity functions over the expected ranges of concentration and temperature yields a model for the fluorescent power output, P_f shown in figure 2. The operating envelope for the system is illustrated as the white box in figure 2, below the saturation line, with reference conditions marked in red. The general model was partially validated against specific experimental measurements by Iida & Ando [45], with caveats and discussion provided in A. Note that while the absolute reference values reported in figure A1 are different than those used in figure 2, only the trend in relative variations is what is being validated, which shows no strong dependence on the reference [60]. For a fixed temperature, P_f increases with C, as the quantity of fluorescent material increases. For a fixed concentration, P_f decreases with T as quenching reduces the fluorescent output [49].

The dependence of fluorescent power on both temperature and concentration means that a given fluorescent power measurement does not map uniquely to a given tracer concentration; rather a variety of different tracer concentrations could produce the same power output at different temperatures. The only way to unambiguously identify concentration from iodine LIF measurements is to hold temperature fixed. All previous studies attempting to infer concentration from iodine LIF recognized this problem [60] and assumed that the temperature was 'constant' [56, 59]. However, they did not report precisely how sensitive to temperature the fluorescent power measurement is, and thus what level of temperature stability control is truly required in order to justify the assumption that the temperature is effectively constant.

4. Temperature sensitivity of concentration measurements

The goal of quantitative iodine LIF is to measure small changes in concentration, dC, which could represent spatial or temporal variations. At fixed temperature, these small concentration variations would result in small variations in the fluorescent power, dP_f, but in a non-isothermal system, temperature variations, dT, will also contribute to the fluorescent power fluctuations. From equation (8), we develop relations for the relative sensitivity of the fluorescent power, dP_f/P_f, as a function of the relative fluctuations of T and C about their reference points, given by:

$$\frac{dP_f}{P_f}=\left[S_1(T,C)+S_2(T,C)\right]\frac{dT}{T}+S_3(T,C)\frac{dC}{C} \tag{10}$$

where the functions S_j represent the effects of the fluorescent efficiency and absorptivity, given by:

$$S_1(T,C)=\frac{d\log\Phi}{d\log T},\quad S_2(T,C)=\frac{d\log\epsilon}{d\log T},$$
$$S_3(T,C)=\epsilon Cl\frac{\log(10)\,10^{-\epsilon Cl}}{1-10^{-\epsilon Cl}} \tag{11}$$

The S_1 and S_2 terms exhibit weak temperature dependence compared to S_3, further suggesting that the precise functional variation of $\Phi(T)$ and $\varepsilon(T)$ will not strongly affect the analysis,

and representative values should be sufficient to describe general trends.

The sensitivity relation (equation (10)) is plotted in figure 3(a) for $\pm$ 1% relative variations in concentration and temperature. A given variation in fluorescent power, dP_f/P_f, detected by a camera, could be explained by a unique variation in tracer concentration, dC/C, under truly isothermal conditions, $dT/T = 0$. But, if there actually exists a finite temperature variation, $dT/T \neq 0$, then the false assumption that $dT/T = 0$ will result in an incorrect inference of the concentration variation, as illustrated in cartoon form in figure 3(b): each point along the measured dP_f/P_f isoline represents a unique combination of $(dC/C, dT/T)$, and thus the assumption about the unknown temperature variations in a system will dictate the inferred concentration variations. In order to employ iodine LIF for concentration measurement, we need to ascertain the maximum allowable temperature variation, dT/T, such that the fluorescent power variation is explained by changes in concentration and not changes in temperature, to some desired degree of confidence.

5. Concentration measurements confounded by temperature variations

The primary concern with unknown temperature variations in the flow is that the actual concentration variation, dC/C, will differ from the value inferred from the fluorescent power assuming isothermal conditions, $dC/C\big|_T$. The maximum relative error tolerance, α, between these two quantities can be bounded as:

$$\alpha \leq \left| \left(\frac{dC}{C}\bigg|_T - \frac{dC}{C} \right) \right| \Big/ \left| \frac{dC}{C}\bigg|_T \right| \tag{12}$$

Thus the sensitivity question can be phrased: given a fixed fluorescent detectability, dP_f/P_f, and a desired concentration measurement resolution (assuming isothermal conditions),$dC/C\big|_T$, what is the maximum tolerable temperature variation, dT/T, that does not exceed the relative error level α?

Under isothermal conditions, the fluorescent power variation is

$$\frac{dP_f}{P_f}\bigg|_T = S_3 \frac{dC}{C}\bigg|_T, \tag{13}$$

and equating this with the fluorescent power variation under actual conditions, given by equation (10), yields:

$$\frac{dC}{C}\bigg|_T - \frac{dC}{C} = \frac{S_1 + S_2}{S_3}\frac{dT}{T}. \tag{14}$$

Taking the magnitude of the difference between the two concentration measurements and substituting the definition of

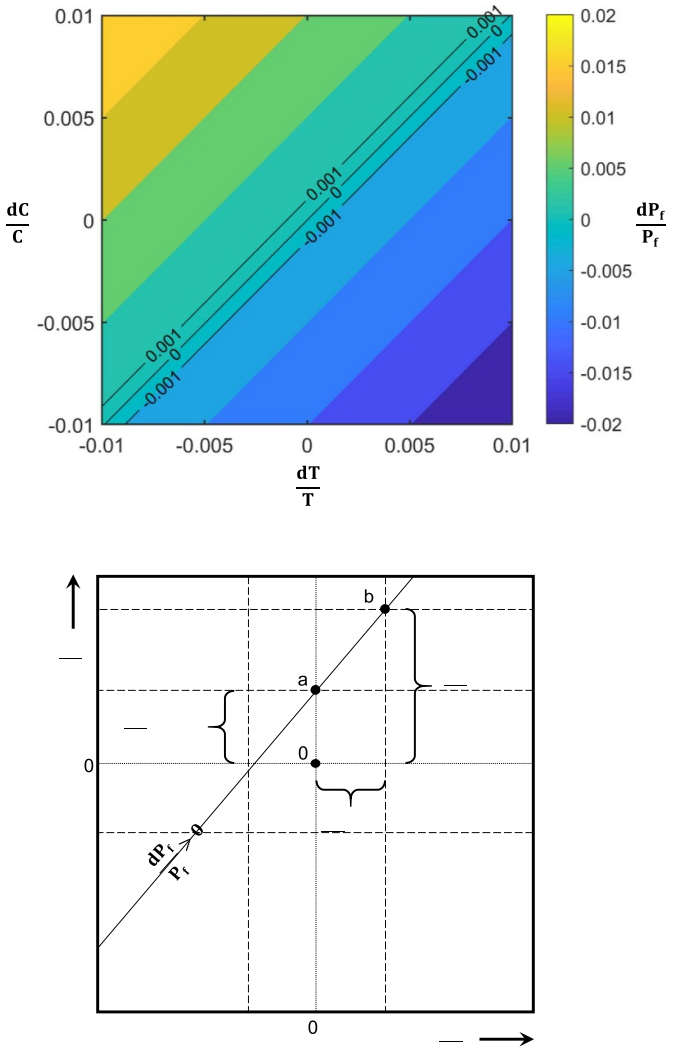

Figure 3. (a) The variation of relative fluorescence power (dP_f/P_f) with relative concentration (dC/C) and relative temperature (dT/T) at reference concentration $C_r = 0.0015$ mol m^{-3} and temperature $T_r = 295$ K. (b) A cartoon illustrating the difference between the concentration variation that would be inferred assuming isothermal conditions, at point **a**, with the true concentration variation taking into account temperature variations, at point **b**, for a single measurement of fluorescence power variation.

the relative error tolerance, α, yields a constraint on the temperature variations:

$$\left| \frac{dT}{T} \right| \leq \alpha \left| \frac{S_3}{S_1 + S_2} \right| \left| \frac{dC}{C}\bigg|_T \right| \tag{15}$$

Figure 4 displays the maximum tolerable temperature variations, dT/T, for a desired relative error tolerance, α, and ideal (isothermal) concentration resolution, $dC/C\big|_T$. For example, to measure 1% relative variations in concentration with relative error $\alpha = 5\%$, the maximum allowable temperature fluctuations in the system are only 0.04% of the system reference temperature.

For illustration, the relative error analysis can then be applied to the experimental case of Iida & Ando [45] who used

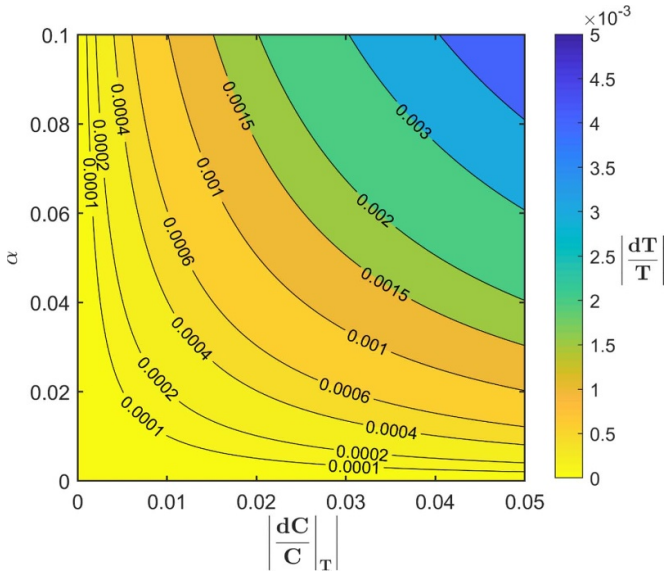

Figure 4. Variation of relative temperature stability requirements, $|dT/T|$, for different error tolerances, α, and isothermal concentration variations, $|(dC/C)|_T|$.

iodine LIF to perform concentration measurements in a turbulent jet. Their camera had 256 gray scale levels to identify the flow field with a maximum molar concentration of of 30% iodine, resulting in an approximate $dC/C\big|_T = 0.001\,3$. To maintain a relative error $\alpha = 5\%$, the maximum relative temperature variation allowed is $dT/T = 0.006\,4\%$, resulting in an absolute temperature variation constraint of $\pm$ 0.02 K about their reference temperature of $T_r = 295$ K, which is exceedingly difficult to achieve for laboratory scale experiments. Indeed, even in quiescent air in a typical laboratory, variations of 0.5–3 K are expected, which translates to $dT/T \approx 0.2$–1% about a reference temperature of 295 K. [62]. Moreover, Iida & Ando [45] utilized hot sonic injectors and thus significant temperature variations are expected when the jet, with fixed nozzle temperature of 333 K, exhausts to the ambient atmosphere at 300 K. Stated in reverse, with a relative temperature variation, defined between the nozzle and ambient temperatures, of $dT/T \approx 10\%$, the relative error predicted for their concentration measurements is $\alpha \approx 78\%$. In other words, the measured fluorescent power variations are mostly due to temperature variations and not concentration variations. Practically speaking, this suggests that the iodine vapor acts as a temperature indicator in systems with such high temperature variations, and extraordinary care should be take in interpreting LIF measurements.

For a modest precision requirement, with relative error $\alpha = 5\%$, the relative temperature stability requirements in most flow systems tend to be an order of magnitude stricter than the desired concentration resolution. For room temperature laboratory systems, this results in an impractical demand for temperature control or, at best, a relative error in concentration measurements exceeding 10%. For heated systems or systems with significant temperature variations, this predicts a nearly impossible temperature uniformity constraint.

6. Conclusions

The fluorescent emission power from iodine LIF depends on both the concentration of the iodine tracer and the temperature of the system. Because of this dual dependence, tracer concentration measurements can be highly confounded by even relatively small temperature variations in the system. By modeling the fluorescent emission in a typical iodine LIF scenario, common to many engineering laboratories, an expression was derived to relate the constraints on temperature uniformity in a system needed in order to measure a given variation in tracer concentration to within a fixed relative error. The temperature variation constraint was found to be roughly an order of magnitude finer than the desired, relative, concentration measurement resolution, and thus iodine LIF should not be used for concentration inference except in highly temperature-controlled environments.

Acknowledgment

The authors acknowledge the support given in part by the Technion Fine Fellowship, and thank the anonymous referees for helpful suggestions regarding appropriate caveats to this generalized modeling approach.

Appendix A. Validation of P_f Model

In order to validate the general fluorescence power prediction (P_f) from equation (8) using the absorptivity model from equation (9), two experimental cases from Iida & Ando [45] were considered: (a) P_f measurements at a constant $T = 323$ K with He as the carrier gas for different C between 0.075–0.15 mol m^{-3}; (b) P_f measurements at a constant $C = 0.052$ mol m^{-3} (C_s at $T = 313$ K) with He as the carrier gas for different T between 315–340 K. The authors represented the fluorescence signal in-terms of luminescence intensity (J, W m^{-2}). In our model, the fluorescence signal is given in terms of power (P_f, W). In order to convert the power to luminescence intensity, we use the reference model that the authors had used which requires light intensity (I, counts) as an input along with the camera's gamma (γ) value (where we fitted the unreported value of γ using the typical range for a generic, modern high-speed camera). The monochromatic radiation luminescence of a black body furnace at 1800 K given by Planck's formula has been used to convert their reported values of luminescence intensity to counts used in their reference model:

$$\frac{J}{J_0} = \left(\frac{I}{I_0}\right)^{\gamma}, \tag{A1}$$

where J is the monochromatic radiation luminance from the objects, J_0 is monochromatic radiation luminance from blackbody furnace at 1800 K, I is the intensity counts registered by the CCD/CMOS sensor from the objects, I_0 is the intensity counts registered by the CCD/CMOS sensor from the blackbody furnace at 1800 K, and γ is the gamma value of CCD camera system.

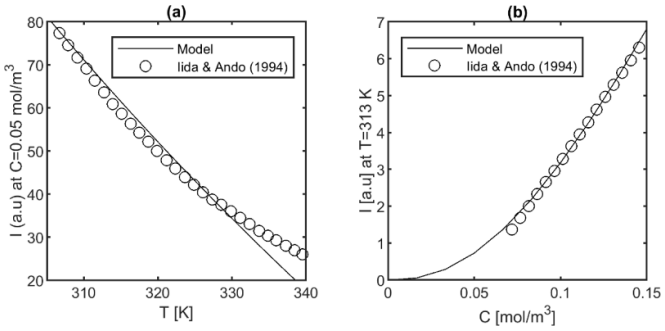

Figure A1. Validation of present model with the experimental cases of Iida & Ando [45]. (a) Fluorescence intensity I (a.u) variation with temperature (T) at a constant concentration (C) of 0.05 mol m^{-3}; (b) fluorescence intensity I (a.u) variation with concentration (C) at a carefully controlled constant temperature (T) of 313 K.

Iida & Ando [45] do not report the specification of their camera, hence for the validation exercise, we assumed the characteristics of a generic 12-bit high-speed CMOS camera with a constant $\gamma = 2.4$ and a sensitivity of 20 counts/μW. In reality, γ varies with incoming light intensity and may require more detailed, system-specific modeling, although the constant γ approximation is widely applicable for modern, high-speed cameras. Similarly, the present modeling framework does not include other system-specific optical efficiency terms that result from the particular placement of a camera in a given experiment, the laser fluctuations specific to a particular make of laser, transmission losses due to the particular choice of optics, and fluorescence signal quenching from the particular transmission medium. All of these experiment-specific features could be easily added to this general modeling framework by the researcher in the field, in order to adapt the predictions to a specific experiment. However, for the purpose of developing an analytical framework for approaching the sensitivity analysis, these details were not included, and the simplified model framework was compared to previously reported experiments, which used He as a carrier gas, by recalculating a plot similar to figure 2 with this carrier gas, as a test of robustness. The final validation of the present analysis with these experiments is plotted in figure A1, where the relative variations are captured by the slope, without regard to the arbitrary reference values. The small deviation in the slope between the model and experiments in figure A1(a) is likely a result of the uncertainty in experimental measurements, and the simplified modeling functions assumed for the unreported parameters, noted above. But, considering the simplifying assumptions, the modeling framework appears quite robust to these experiment-specific uncertainties over a wide range of near-'room-temperature' lab situations.

ORCID iD

S K Karthick https://orcid.org/0000-0003-1285-9771

References

[1] Daily J W 1976 Laser induced fluorescence as an engineering tool *Proc. SPIE* **82** 146–51
[2] Miles R B and Lempert W R 1997 Quantitative flow visualization in unseeded flows *Ann. Rev. Fluid Mech.* **29** 285–326
[3] Yang Z, Xin Y, Peng J and Jianlong Zhang 2019 Laser technology and its applications *Quantitative Planar Laser-Induced Fluorescence Technology* Yufei M (Rijeka: IntechOpen) https://doi.org/10.5772/intechopen.79702
[4] Wang K C, Smith O I and Karagozian A R 1995 In-flight imaging of transverse gas jets injected into compressible crossflows *AIAA J.* **33** 2259–63
[5] Paul P H and Hanson R K 1990 Applications of planar laser induced fluorescence diagnostics to reacting flows *26th Joint Propulsion Conf.* AIAA https://doi.org/10.2514/6.1990-1848
[6] Rapagnani N L and Davis S J 1979 Laser-induced i2 fluorescence measurements in a chemical laser flowfield *AIAA J.* **17** 1402–4
[7] Rapagnani N L and Davis S L 1985 Laser-induced fluorescence: A diagnostic for fluid mechanics: Laser-induced fluorescence opens a new field of nonintrusive flowfield diagnostics *Lasers Appl.* **4** 127–31
[8] Karthick S K, Rao S M V, Jagadeesh G and Reddy K P J 2017 Passive scalar mixing studies to identify the mixing length in a supersonic confined jet *Exp. Fluids* **58** 20
[9] Hiller W J and Schmidt-Ott W D 1977 Visualization of low density gas-jets by laser induced fluorescence *ICIASF '77-Int. Congress on Instrumentation in Aerospace Simulation Facilities* 68–73
[10] Teshima K, Moriya T and Mori T 1984 Visualization of a free jet by a laser induced fluorescence method *Aeronautical Space Sci. Japan* **32** 309–12
[11] Hanson R K 1988 Planar laser-induced fluorescence imaging *J. Quant. Spectrosc. Radiat. Transfer* **40** 343–62
[12] Telle H H, Urena A G and Donovan R J 2007 *Laser Chemistry: Spectroscopy Dynamics and Applications* (Chichester: Wiley)
[13] Sauer M, Hofkens J and Enderlein J 2011 *Handbook of Fluorescence Spectroscopy and Imaging* (Wiley-VCH Verlag GmbH & Co. KGaA) Weinheim https://doi.org./10.1002/9783527633500
[14] Hassa C, Paul P H and Hanson R K 1987 Laser-induced fluorescence modulation techniques for velocity measurements in gas flows *Exp. Fluids* **5** 240–6
[15] Lee T, Jeffries J B, Hanson R K, Bessler W G and Schulz C 2004 Carbon dioxide uv laser-induced fluorescence imaging in high-pressure flames *42nd AIAA Aerospace Sciences Meeting and Exhibit* Reno, Nevada AIAA 177–82
[16] Alden M, Hertz H M, Svanberg S and Wallin S 1984 Imaging laser-induced fluorescence of oxygen atoms in a flame *Appl. Opt.* **23** 3255–7
[17] Cheung B H and Hanson R K 2010 Cw laser-induced fluorescence of toluene for time-resolved imaging of gaseous flows *Appl. Phys. B: Lasers Opt.* **98** 581–91
[18] Lozano A, Yip B and Hanson R K 1992 Acetone: a tracer for concentration measurements in gaseous flows by planar laser-induced fluorescence *Exp. Fluids* **13** 369–76
[19] Weiland K J R, Wise M L and Smith G P 1993 Laser-induced fluorescence detection strategies for sodium atoms and compounds in high-pressure combustors *Appl. Opt.* **32** 4066–73
[20] Zucco M, Robertsson L and Wallerand J 2013 Laser-induced fluorescence as a tool to verify the reproducibility of iodine-based laser standards: A study of 96 iodine cells *Metrologia* **50** 402–8

[21] McDaniel J C 1982 Transverse gas jet injection behind a rearward-facing step investigation of laser induced iodine fluorescence for the measurement of density in compressible flows *PhD Thesis*, Stanford University 129

[22] Hiller B and Hanson R K 1990 Properties of the iodine molecule relevant to laser-induced fluorescence experiments in gas flows *Exp. Fluids* **10** 1–11

[23] Lai M C, Jeng S M and Faeth G M 1986 Structure of turbulent adiabatic wall plumes *ASME: J. Heat Trans.* **108** 827–34

[24] Muruganandam T M, Lakshmi S, Ramesh A A, Viswamurthy S R, Sujith R I and Sivaram B M 2002 Mixing of transversely injected jets into a crossflow under low-density conditions *AIAA J.* **40** 1388–94

[25] Wu Y, Xu W, Lei Q and Single-shot L M 2015 volumetric laser induced fluorescence (vlif) measurements in turbulent flow seeded with iodine *Opt. Express* **23** 11

[26] Wu Y, Xu W and Ma L 2018 Kilohertz vlif (volumetric laser induced fluorescence) measurements in a seeded free gas-phase jet in the transitionally turbulent flow regime *Opt. Lasers Eng.* **102** 52–8

[27] Xu W, Liu N and Ma L 2018 Super resolution plif demonstrated in turbulent jet flows seeded with i2 *Opt. Laser Technol.* **101** 216–22

[28] Inoue M, Masuda M, Furukawa M and Muraishi T 1995 Diagnosis of a three-dimensional transonic flow by measuring temperature distribution with a laser-induced fluorescence technique *Trans. Japan Soc. Mech. Eng.* B **61** 3230–5

[29] Cenkner Jr A A and Driscoll R J 1982 Laser-induced fluorescence visualization on supersonic mixing nozzles that employ gas-trips *AIAA J.* **20** 812–19

[30] Zagidullin M V, Torbin A P and Chernyshov A A 2015 Gas flow visualization using laser-induced fluorescence *Procedia Eng.* **106** 92–6

[31] Exton R J, Balla R J, Shirinzadeh B, Hillard M E and Brauckmann G J 1999 Flow visualization using fluorescence from locally seeded i2 an arf excimer laser *Exp. Fluids* excited by **26** 335–9

[32] McDaniel J C, Cordoni J R, Alkandry H and Boyd I D 2013 Propulsion deceleration studies using planar laser induced iodine fluorescence and computational fluid dynamics *J. Spacecr. Rockets* **50** 771–80

[33] Ni-Imi T, Fujimoto T, Wakayama K and Ishida T 1992 Method for measurement of temperature in rarefied gas flowusing plif *Trans. Japan Soc. Mech. Eng.* B **58** 3275–9

[34] Fujimoto T, Sato K, Naniwa S, Inoue T, Nakashima K and Niimi T 2001 Visualization of impinging supersonic free jet on a tilt plate by lif and psp *J. Visualization* **4** 151–8

[35] McDaniel J C 1984 Nonintrusive pressure measurements with laser-induced iodine fluorescence Nonintrusive pressure measurements with laser-induced iodine fluorescence *Combustion Diagnostics by Nonintrusive Methods* McCay, T Roux, J Reston, VA AIAA **12** 107–31

[36] Ackermann U, Baganoff D and McDaniel J C 1985 Dependence of laser-induced fluorescence on gas-dynamic fluctuations with application to measurements in unsteady flows *Exp. Fluids* **3** 45–51

[37] Hartfield J, Hollo R J, S D and McDaniel J C 1993 Planar measurement technique for compressible flows using laser-induced iodine fluorescence *AIAA J.* **31** 483–90

[38] Lemoine F and Leporcq B 1995 An efficient optical pressure measurement in compressible flows: Laser-induced iodine fluorescence *Exp. Fluids* **19** 150–8

[39] Hasegawa T, Miyawaki K, Yamaguchi S and Ohiwa N 1989 Concentration measurement in a jet by laser-induced fluorescence method *Nihon Kikai Gakkai Ronbunshu, B Hen/Trans. Japan Soc. Mech. Eng.* B **55** 1458–62

[40] Niimi T, Fujimoto T and Taoi N 1993 Analysis of flow fields of interacting parallel supersonic free jets *Trans. Japan Soc. Mech. Eng.* B **59** 3325–30

[41] Donohue J M and McDaniel J C 1996 Jr. Computer-controlled multiparameter flowfield measurements using planar laser-induced iodine fluorescence *AIAA J.* **34** 1604–11

[42] Handa T, Masuda M and Matsuo K 2005 Three-dimensional normal shock-wave/boundary-layer interaction in a rectangular duct *AIAA J.* **43** 2182–7

[43] Takagi T, Kondo T, Komiyama M and Shintani Y 1988 Continuous and simultaneous measurements of concentration and velocity by laser-induced fluorescence and ldv *Trans. Japan Soc. Mech. Eng.* B **54** 1179–82

[44] Asada N, Matsui H and Nakajima S 1991 An approach to gas flow measurement by laser induced fluorescence. application to chemical vapor deposition *Opt. Commun.* **82** 267–72

[45] Iida N and Ando A 1994 Concentration measurement in a transient gas jet using the laser-induced fluorescence method *JSAE Rev.* **15** 123–31

[46] Dai Z, Tseng L-K and Faeth G M 1994 Structure of round, fully developed, buoyant turbulent plumes *J. Heat Transfer* **116** 409–17

[47] Vorobieff P, Truman C R, Ragheb A M, Elliott G S, Laystrom-Woodard J K, King D M, Carroll D L and Solomon W C 2011 Mixing enhancement in a multi-stream injection nozzle *Exp. Fluids* **51** 711–22

[48] Leenson I A 2005 Sublimation of iodine at various pressures: Multipurpose experiments in inorganic and physical chemistry *J. Chem. Educ.* **82** 5

[49] Masiello T, Vulpanovici N and Nibler J W 2003 Fluorescence lifetime and quenching of iodine vapor *J. Chem. Educ.* **80** 914–17

[50] Smith S H and Mungal M G 1998 Mixing structure and scaling of the jet in crossflow *J. Fluid Mech.* **357** 83–122

[51] Miller V A, Gamba M, Mungal M G and Hanson R K 2013 Single- and dual-band collection toluene plif thermometry in supersonic flows *Exp. Fluids* **54** 1539

[52] Lemoine F and Grisch F 2013 Laser-Induced Fluorescence *Laser Metrology in Fluid Mechanics* Hoboken, NJ Wiley 159-222

[53] Yamaguchi S, Hasegawa T, Miyawaki K and Ohiwa N 1989 Two-dimensional mean concentration measurement in a jet by planar laser-induced fluorescence method *Nihon Kikai Gakkai Ronbunshu, B Hen/Trans. Japan Soc. Mech. Eng.* B **55** 3566–70

[54] Hartfield R J, Hollo S D and McDaniel J C 1994 Experimental investigation of a supersonic swept ramp injector using laser-induced iodine fluorescence *J. Propulsion Power* **10** 129–35

[55] Hartfield R J and Bayley D J 1996 Experimental investigation of angled injection in a compressible flow *J. Propulsion Power* **12** 442–5 Jrand

[56] Lai M C and Faeth G M 1987 A combined laser-doppler anemometer/laser induced fluorescence system for turbulent transport measurements *Trans. ASME* **109** 254–6

[57] Dai Z, Tseng L K and Faeth G M 1995 Velocity statistics of round, fully developed, buoyant turbulent plumes *J. Heat Transfer* **117** 138–45

[58] Kido A, Ogawa H and Miyamoto N 1992 Quantitative processing to calculate mixture strength in jet streams by laser-induced fluorescence of ambient-gas (lifa method) *Nihon Kikai Gakkai Ronbunshu, B Hen/Trans. Japan Soc. Mech. Eng.* B **58** 3201–7

[59] Kido A, Ogawa H, Mayamoto N and Sano T 1993 Quantitative analysis of the gas entrainment process of intermittent gas jets with laser-induced fluorescence of ambient gas(lifa) *Trans. Japan Society Mech. Eng.* B **59** 865–71

[60] Kido A, Ishikawa S, Ogawa H and Miyamoto N 1998 Simultaneous measurements of concentration and temperature distribution in unsteady gas jets by laser-induced fluorescence of ambient gas *Nihon Kikai Gakkai Ronbunshu, B Hen/Trans. Japan Society Mech. Eng.* B **64** 1247–53

[61] Compton R N and Duncan M A 2015 *Laser Experiments for Chemistry and Physics* (Oxford: Oxford University Press) https://doi.org.10.1093/acprof:oso/9780198742975.001.0001

[62] Melikov A K, Krüger U, Zhou G, Madsen T L and Langkilde G 1997 Air temperature fluctuations in rooms *Building Environ.* **32** 101–14